Experimental Neurology 320 (2019) 113007

Contents lists available at ScienceDirect

Experimental Neurology

journal homepage: www.elsevier.com/locate/yexnr

Research Paper

Delayed recanalization at 3 days after permanent MCAO attenuates neuronal apoptosis through FGF21/FGFR1/PI3K/Caspase-3 pathway in rats

Wen Zheng[a,b], Nathanael Matei[b], Jinwei Pang[b], Xu Luo[b], Zhi Song[a], Jiping Tang[c], John H. Zhang[b,c,*]

[a] Department of Neurology, The Third Xiangya Hospital, Central South University, Changsha, Hunan 410013, China
[b] Department of Anesthesiology, Neurosurgery and Neurology, School of Medicine, Loma Linda University, Loma Linda, CA 92354, USA
[c] Department of Physiology and Pharmacology, Basic Sciences, School of Medicine, Loma Linda University, Loma Linda, CA 92354, USA

ARTICLE INFO

Keywords:
Delayed recanalization
Permanent MCAO
Ischemia/reperfusion injury
FGF21
Neuronal apoptosis

ABSTRACT

Reperfusion exceeded time window may induce ischemia/reperfusion injury, increase hemorrhagic transformation, and deteriorate neurological outcomes in ischemic stroke models. However, the increasing clinical evidences supported that reperfusion even within 6–24 h may salvage ischemic tissue and improve neurological outcomes in selected large vessel occlusion patients, without inducing serious ischemia/reperfusion injury and hemorrhagic transformation. The underlying molecular mechanisms are less clear. In present study, we demonstrated that delayed recanalization at 3 days after permanent middle cerebral artery occlusion (MCAO) decreased infarct volumes and improved neurobehavioral deficits in rats, with no increasing animal mortality and intracerebral hemorrhage. Meanwhile, we observed that endogenous neuroprotective agent fibroblast growth factor 21 (FGF21) significantly increased in serum after MCAO, but which did not synchronously increase in penumbra due to permanent MCAO. Recanalization dramatically increased the endogenous FGF21 expression on neurons in penumbra after MCAO. We confirmed that FGF21 activated the FGFR1/PI3K/Caspase-3 signaling pathway, which attenuated neuronal apoptosis in penumbra. Conversely, knockdown of FGFR1 via FGFR1 siRNA abolished the anti-apoptotic effects of FGF21, and in part abrogated beneficial effects of recanalization on neurological outcomes. These findings suggested that delayed recanalization at 3 days after MCAO improved neurological outcomes in rats via increasing endogenous FGF21 expression and activating FGFR1/PI3K/Caspase-3 pathway to attenuate neuronal apoptosis in penumbra. Delayed recanalization at 3 days after ischemic stroke onset may be a promising treatment strategy in selected patients.

1. Introduction

Ischemic stroke is still the leading cause of death, long-term disability, and dementia in adult humans worldwide (Kim et al., 2018; Lopez-Morales et al., 2018; Wang et al., 2018; Sun et al., 2018). A significant decline of life quality might occur in patients who survived an ischemic stroke (Wang et al., 2018; Gopalakrishnan et al., 2019; Otero-Ortega et al., 2018). In recent years, primary improvements in the treatment of acute ischemic stroke involve thrombolysis with recombinant tissue-type plasminogen activator (rt-PA) and endovascular thrombectomy (Wang et al., 2018). However, these beneficial recanalization treatments have been limited in most patients due to the strict therapeutic time window (Lopez-Morales et al., 2018). In patients with occlusion of internal carotid artery (ICA) or the first segment of the middle cerebral artery (MCA), rt-PA should be administered within 4.5 h (Kim et al., 2018), and endovascular thrombectomy should be initiated within 6 h (Albers et al., 2018). Of the approximately 300,000 ischemic stroke patients with large vessel occlusion (LVO) in US annually, up to 15% patients are treated with tPA (Gonzalez et al., 2013), and only 2.6–4% patients are treated with endovascular embolectomy (Rai, 2015; McBride and Zhang, 2017), with only a total of 3.65–9% patients occurred recanalization (McBride and Zhang, 2017). Therefore, it is the fact that only a minority of ischemic stroke patients might benefit from the recanalization therapeutic strategy (Lopez-Morales et al., 2018). Furthermore, the clinical therapeutic options are actually limited to benefit patients who missed the time window after ischemic stroke (Kim et al., 2018). Due to this intractable problem to patients and neurological clinicians, it is necessary to develop a promising therapeutic strategy for ischemic stroke (Kim et al., 2018).

It is worth noting that spontaneous recanalization may occur in

* Corresponding author at: Department of Anesthesiology, Neurosurgery and Neurology, School of Medicine, Loma Linda University, Loma Linda, CA 92354, USA.
E-mail address: johnzhang3910@yahoo.com (J.H. Zhang).

https://doi.org/10.1016/j.expneurol.2019.113007
Received 12 February 2019; Received in revised form 6 June 2019; Accepted 4 July 2019
Available online 08 July 2019
0014-4886/

about 20% (or up to 45%) LVO stroke patients who do not receive thrombolytics or endovascular therapies (McBride and Zhang, 2017; Cloft et al., 2009; Chen et al., 2015; Albers et al., 2018). Specifically, spontaneous recanalization occurs in 21.4% middle cerebral artery occlusion (MCAO) patients within 24 h after ischemic stroke and in 52.7% MCAO patients after a week (Rha and Saver, 2007; Zanette et al., 1995; Mao et al., 2017), usually associated with improving prognosis (McBride and Zhang, 2017; Mao et al., 2017). Our previous study also demonstrated that delayed recanalization at 3, 7, and 14 days (d) after stroke restored cerebral blood flow, reduced infarct volume, and improved neurological outcomes in permanent MCAO (pMCAO) rats (McBride et al., 2018). Recently, two large clinical randomized controlled trials also showed that thrombectomy improved neurological outcomes even in 6–24 h after stroke onset in selected large vessel occlusion (LVO) patients (Albers et al., 2018; Nogueira et al., 2018). Therefore, delayed recanalization may be an alternative promising therapeutic strategy for most patients who missed time window after stroke (Kelly and Holloway, 2018). While, it is well known that reperfusion exceeded time window will only exacerbate ischemia/reperfusion injury, increase hemorrhagic transformation, and deteriorate neurological outcomes (McBride and Zhang, 2017). So, it is very interesting and puzzled that delayed recanalization improves the prognosis and does not induce serious ischemia/reperfusion injury in a part of ischemic stroke patients. The underlying molecular mechanisms remain unclear up to now.

Following ischemia/reperfusion injury, a number of protective agents will be up-regulated in serum. Fibroblast growth factor 21 (FGF21) is a multifunctional metabolic stress hormone and predominately expressed in liver. Multiple evidences showed that hepatic and cardiac ischemic injury induced FGF21 secreted promptly from liver, pancreas, heart, kidney, skeletal muscles, and adipose tissue, via activating the protein kinase RNA-like endoplasmic reticulum kinase (PERK)/eukaryotic initiation factor 2α (eIF2α)/activating transcription factor 4 (ATF4) axis (Luo et al., 2017; Salminen et al., 2017a). Recent researches indicated that FGF21 attenuated cell apoptosis to reduce ischemia/reperfusion injury in liver, heart, and H9c2 cells via activating fibroblast growth factor receptor 1 (FGFR1) and downstream signaling pathways (Ye et al., 2016; Liu et al., 2013; Cong et al., 2013).

We supposed that serum FGF21 may also increase after ischemic stroke and contribute to attenuate relevant brain injury. However, it was reported that endogenous FGF21 level significantly decreased in ischemic core after stroke, for all that FGF21 mRNA levels were not affected (Wang et al., 2016). Considering FGF21 predominately secreted from several tissues outside brain, the blocking of cerebral blood flow after LVO may prevent serum FGF21 expressing in ischemic core. In this study, we hypothesize that delayed recanalization (at 3 d after MCAO) may restore cerebral blood flow and up-regulate endogenous FGF21 expression in penumbra, which contribute to attenuating neuronal apoptosis and improving neurological outcomes through FGF21/FGFR1/phosphoinositide 3-kinase (PI3K)/Caspase-3 signaling pathway.

2. Materials and methods

2.1. Animals

The experimental protocols in this study were all approved by the Institutional Animal Care and Use Committee of Loma Linda University and accorded with the National Institutes of Health (NIH) guide for the care and use of laboratory animals. Two hundred and thirty-four adult male Sprague–Dawley (SD) rats, weighing 260–280 g, were assigned to either sham or MCAO surgery. All rats were housed in a humidity and temperature-controlled environment with regular light/dark cycle and free access to food and water.

2.2. pMCAO model

To establish pMCAO models and induced focal ischemia, the right MCA of rats were occluded using the intraluminal technique as previously described (Liang et al., 2014; Gubskiy et al., 2018). All rats were anesthetized firstly by intraperitoneal injection with ketamine (80 mg/kg) and xylazine (10 mg/kg). Following subcutaneous injection of Atropine at a dose of 0.1 mg/kg. The right common carotid artery (CCA), external carotid artery (ECA), and ICA were exposed in sequence. After ECA was ligatured, a nylon suture with a silicon tip was planted into the ICA via proximal ECA to occlude the MCA. After surgery, the incision was closed with sutures. All rats were recovering from anesthesia in a 37 °C container separately. The suture was withdrawn from a part of rats to establish MCA recanalization at 3 d after MCAO. Rats in sham were subjected the same procedures apart from MCA occlusion and recanalization.

2.3. Study design

All survival rats divided randomly into pMCAO group or recanalization after MCAO (rMCAO) group following neurological scores test at 3 d after MCAO.

2.3.1. Experiment I

Including the sham group (n = 6), eight groups were established in experiment I. After neurological scores test to exclude the very terrible or perfect rats at 3d after MCAO, Rats (modified Garcia score ranging from 6 to 9) were randomly divided into seven groups (pMCAO 3d, pMCAO 4d, rMCAO 4d, pMCAO 10d, rMCAO 10d, pMCAO 30d, and rMCAO 30d). Western blot was performed to determine the time course of endogenous FGF21 and FGFR1 expression in penumbra (n = 6). Serum FGF21 was tested by ELISA (n = 6). Immunofluorescence staining was performed to identify the colocalization of FGF21 and FGFR1 with neurons at the peak of FGF21 expression (n = 3, three sections per slice were photographed).

2.3.2. Experiment II

To evaluate the effects of recanalization on infarct and neurological outcomes, infarct volume (n = 6), modified Garcia (n = 9), and beam walking scores (n = 9) were assessed in eight groups (sham, pMCAO 3d, pMCAO 4d, rMCAO 4d, pMCAO 10d, rMCAO 10d, pMCAO 30d, and rMCAO 30d). Morris water maze was performed at 30 d after MCAO to evaluate spatial learning and memory capacity (n = 9). Fluoro-Jade C (FJC) staining and terminal deoxynucleotidyl transferase dUTP nick end labeling (TUNEL) staining were performed to test the cell death at 4 d after MCAO (i.e. 1 d after recanalization, n = 3, three sections per slice were photographed).

2.3.3. Experiment III

To explore the underlying mechanisms of FGF21 mediated anti-apoptosis effects after recanalization, five groups were established, including sham, pMCAO, rMCAO, scrambled siRNA (Scr siRNA), and FGFR1 siRNA. Scrambled siRNA or FGFR1 siRNA GFP lentivirus were administered via intracerebroventricular injection at 1 h before MCAO. Recanalization was conducted at 3 d after MCAO. Immunofluorescence staining was performed to identify whether FGFR1 siRNA GFP lentivirus successfully transduced neurons at 4 d after pretreatment (n = 3). Western blot was performed at 4 d (i.e. 1 d after recanalization) after MCAO to test the expression of FGF21 and downstream proteins (n = 6). Infarct volume, modified Garcia Score, and meam walking scores were performed at 10 d after MCAO to evaluate the neurological outcomes (n = 6)

2.4. Enzyme linked immunosorbent assay (ELISA)

ELISA was performed to test the serum FGF21 expression. Blood

samples were collected into a serum separator tube. After clot formation and centrifuging at 2000 × *g* for 10 min, serum samples were collected and stored at −20 °C. All reagents, working standards, and samples were prepared according to the manufacturer's instruction manuals of rat FGF21 ELISA kit (ab223589, Abcam, Cambridge, MA, USA). All 96-well plates were precoated with rat FGF21 antibodies. 50 µl of serum sample or standard were added to appropriate wells, then 50 µl of the antibody cocktail were added to each well. After incubating for 1 h on a plate shaker (400 rpm) at room temperature and washing each well with 3 × 350 µl 1 × wash buffer PT, 100 µl of TMB substrate was added to each well and incubate for 10 min in the dark on a plate shaker (400 rpm). At last, 100 µl of stop solution was added to each well followed by plate shaking for 1 min to mix and recording optical density at 450 nm. Results were calculated and interpreted according to the instruction manual.

2.5. Intracerebroventricular injection of siRNA

To investigate the potential molecular mechanism of the FGF21 anti-apoptosis effect, intracerebroventricular injection of FGFR1 siRNA GFP lentivirus was performed at 1 h before MCAO to knockdown FGFR1 expression in neurons. The FGFR1 siRNA GFP lentivirus eliminates any possible recombination events that can occur by a dual convergent promoter system, where the sense and antisense strands of the siRNA are expressed by two different promoters rather than in a hairpin loop. Intracerebroventricular injection was conducted as previously described (Yu et al., 2018). Rats were anesthetized by 2.5% isoflurane and were placed in stereotaxic apparatus. The tip of 10 µl Hamilton syringe (Microliter 701; Hamilton Company, Reno, NV, USA) drilled into the right lateral ventricle via a burr hole. The stereotactic site of intracerebroventricular injection was relative to bregma: 1.5 mm posterior, 0.9 mm right lateral, and 3.3 mm depth. 5 µl of either scrambled siRNA GFP lentivirus or FGFR1 siRNA GFP lentivirus (Applied Biological Materials, Richmond, BC, CANADA) was injected 1 h before MCAO. The injection rate was 1 µl/min, and the needle was remained for 5 min after intracerebroventricular injection, and then was withdrawn over 5 min to prevent possible leaking. The burr hole was sealed with bone wax after injection. The incision was closed with sutures, and then rat was followed by MCAO surgery.

2.6. Neurological score evaluation

Modified Garcia score and beam walking test were performed by a blinded investigator as previously described (Garcia et al., 1995; Goldstein and Davis, 1990). The modified Garcia score consists of 6 items (including spontaneous activity, symmetry in the movement of four limbs, forepaw outstretching, climbing, body proprioception, response to vibrissae touch) with a maximum score of 18. Beam walking test bases on a 0–5-point scale. A higher score in two tests accords with a better neurological performance.

2.7. Morris water maze

Morris water maze was performed with blinded strategy at 30 d after MCAO as previously described (Xu et al., 2018; Pu et al., 2016). Each rat was performed 5 trials in every day from 1 d to 5 d. The platform (diameter: 10 cm) was above the water surface and visible at 1 d (cued test). Rats may catch sight of and climb up the platform. Without finding the platform within 60 s, the rat should be guided to climb up the platform and remain on the platform for 10 s (block 1). From 2 d to 5 d (spatial test, blocks 2–5, 1 min each trial), the submerged platform was 1 cm below the water. The platform was removed at 6 d (probe trial), the time spent in the platform-quadrant was identified in trial for 1 min. Swim path, escape latency, swim distance, and the time spent in the platform-quadrant were recorded by a computerized tracking system (Noldus Ethovision; Noldus, Tacoma, WA, USA).

2.8. Assessment of cerebral infarct volume

Triphenyl tetrazolium chloride (TTC) staining only was performed to calculate infarct volume at 3 d, 4 d, and 10 d after MCAO in this study. Rats were anesthetized and perfused with cold phosphate-buffered saline (PBS, 0.1 M, pH 7.4, Sigma-Aldrich, St. Louis, MO, USA). The whole brain was rapidly taken out and sectioned coronally into 2 mm thick slices. Brain slices were incubated in 2% TTC (Sigma-Aldrich, St. Louis, MO, USA) for 15 min and then photographed (Griemert et al., 2018). The infarct area and ipsilateral hemisphere of each brain slice were calculated via ImageJ (ImageJ 1.4; NIH, Bethesda, MD, USA). The brain edema after infarct was rectified by standard methods (whole contralateral hemispheric volume subtracts non-ischemic ipsilateral hemispheric volume). The final results were shown with a ratio of the corrected infarct volume to whole contralateral hemispheric volume (McBride et al., 2016).

Nissl staining was performed to calculated the cerebral infarct volume at 30 d after MCAO. Rats were anesthetized by isoflurane and then perfused by ice cold PBS (100 ml) and 10% formaldehyde solution (100 ml, Sigma-Aldrich, St. Louis, MO, USA). The brains were taken out and immerged in 10% formaldehyde solution for 48 h, and then immersed into 30% sucrose solution for 3 d. Brains were sliced coronally with 20 µm thickness on a freezing microtome (LM3050S; Leica Microsystems, Bannockburn, III, Germany). After sections were completely dried in a 50 °C oven and placed at room temperature for 30 min, they were immerged into 95% Flex (Sigma-Aldrich, St. Louis, MO, USA) for 1 min and 70% Flex for 1 min, respectively. After washing in distilled water for 30 s, the sections were incubated with Cresyl Violet (Sigma-Aldrich, St. Louis, MO, USA) for 1 min, followed by rinsing in distilled water, dehydrating in 100% Flex, and clearing in xylene (Sigma-Aldrich, St. Louis, MO, USA). The sections were covered by slips with DPX Mountant (Sigma-Aldrich, St. Louis, MO, USA) and observed with light microscopy.

2.9. Immunofluorescence staining

The brain samples were processed as same as the Nissl staining. Brains were sliced coronally with 8 µm thickness on the freezing microtome. Double immunofluorescence staining was performed at 4 d after MCAO as previously described (Wu et al., 2018; Xie et al., 2017; Pang et al., 2018). Brain slices were rinsed by PBS for 3 times (5 min × 3) and permeabilized with 0.3% Triton X-100 (Sigma-Aldrich, St. Louis, MO, USA) for 10 min at room temperature. Subsequently, brain slices were washed by PBS for 3 times (5 min × 3) again and blocked with 5% donkey serum (566,460, Sigma-Aldrich, St. Louis, MO, USA) for 2 h, followed by incubating in different primary antibodies at 4 °C overnight: mouse anti-GFAP (1:150, ab16997, Abcam, Cambridge, MA, USA), mouse anti-neuronal nuclei (NeuN, 1:200, ab177487, Abcam, Cambridge, MA, USA), goat anti-Iba-1 (1:100, ab178847, Abcam, Cambridge, MA, USA), rabbit anti-FGF21 (1:100, MBS2027242, MyBioSource, San Diego, CA, USA), rabbit anti-FGFR1 (1:100, ab10646, Abcam, Cambridge, MA, USA), rabbit anti-FGFR1 (phospho Y654, 1:200, ab59194, Abcam, Cambridge, MA, USA). Brain slices were incubated with corresponding fluorescence-conjugated secondary antibodies (1:150, Jackson ImmunoResearch, West Grove, PA) for 2 h at room temperature next day. The slices were observed on a fluorescence microscope (Leica DMi8, Leica Microsystems, Wetzlar, Germany). Three sections per slice were photographed.

2.10. FJC staining

FJC staining was performed to identify degenerating neurons as previously described (Yu et al., 2018). According to the instruction of modified FJC ready-to-dilute staining kit (TR-100-FJ, Biosensis,

A

Time-point	Died rats/Total rats	
	pMCAO	rMCAO
0 ~ 3d	44/148 (29.7%)	
3d	104 rats grouped	
3 ~ 4d	1/18	2/19
4 ~ 10d	5/14	5/14
10 ~ 30d	3/21	2/18
Total (3 ~ 30d)	9/53 (17.0%)	9/51 (17.6%)
Total (0 ~ 30d)	62/148 (41.9%)	

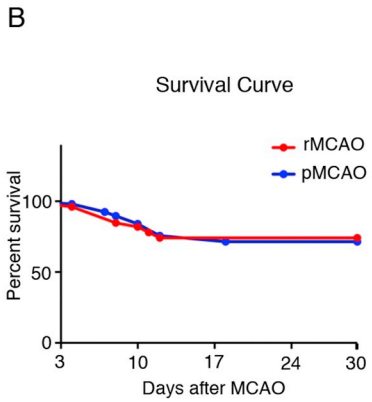

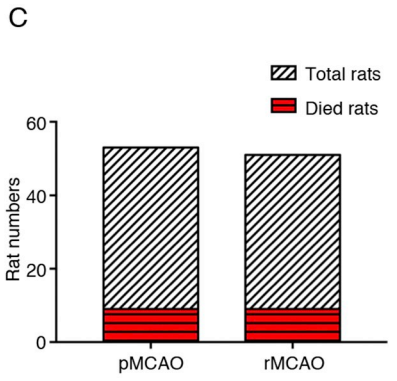

D

Time-point	Hemorrhage rats/Total rats	
	pMCAO	rMCAO
0 ~ 3d	10/44 (22.7%)	
3d	104 rats grouped	
3 ~ 4d	1/18	3/19
4 ~ 10d	3/14	2/14
10 ~ 30d	4/21	2/18
Total (3 ~ 30d)	8/53 (15.1%)	7/51 (13.7%)
Total (0 ~ 30d)	25/148 (16.9%)	

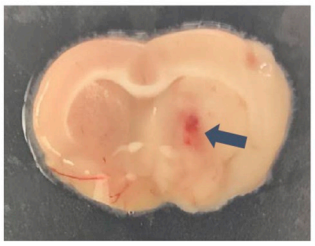

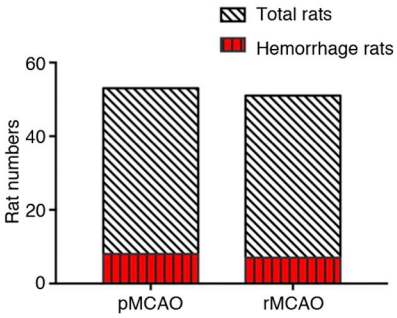

Fig. 1. Animal mortality and intracerebral hemorrhage after MCAO/recanalization. (A) Animal mortality; (B) Survival Curve, n = 53/51, p = .9838, Log-rank (Mantel-Cox) test; (C) Death toll, $p > .05$, n = 53/51, Fisher's exact test; (D) Rate of cerebral hemorrhage; (E) Representative image of hemorrhagic spot in brain slice; (F) Hemorrhage toll, $p > .05$, n = 53/51, Fisher's exact test. pMCAO, permanent middle cerebral artery occlusion; rMCAO, recanalization at 3 d after MCAO; d, day.

Thebarton, South Australia), slides were incubated in mixture of sodium hydroxide (Sigma-Aldrich, St. Louis, MO, USA) and 70% ethanol (Sigma-Aldrich, St. Louis, MO, USA) for 5 min, followed by washing in 70% ethanol for 2 min and in distilled water for 2 min. Subsequently, slides were incubated in 0.06% potassium permanganate (Sigma-Aldrich, St. Louis, MO, USA) solution for 10 min, followed by rinsing in distilled water for 2 min. Slides then were incubated in 0.0001% FJC (MilliporeSigma, Burlington, MA, USA) for 10 min, adding 4′,6-diamidino-2-phenylindole (DAPI, 10236276001, Sigma-Aldrich, St. Louis, MO, USA) and protecting from light. Slides were then rinsed (1 min × 3) in distilled water. After dried at 50–60 °C for 5 min, slides were cleared by immersing in xylene for 1 min and added coverslips with DPX mountant. The slides were visualized in blinded strategy with fluorescence microscope Leica DMi8. FJC-positive neurons (cells/mm^2) were calculated in three sections per slice.

2.11. TUNEL staining

TUNEL staining was performed to quantify of neuronal cell death according to the instruction of in situ cell death detection kit, fluorescein (11684795910, Roche, Sigma-Aldrich, St. Louis, MO, USA). Neuronal marker NeuN staining was performed at the same time. TUNEL-positive (green) cells and NeuN-positive (red) neurons were merged before calculation. The calculation methods of TUNEL positive cells is similar to that of FJC staining.

2.12. Western blots analysis

After TTC staining, the contralateral and ipsilateral cerebrums were frozen in liquid nitrogen immediately, and then stored at −80 °C. Western blot was performed as previously described (Xie et al., 2017; Navarro-Oviedo et al., 2018). Cerebral tissue samples were homogenized with RIPA lysis buffer (sc-24948A, Santa Cruz Biotechnology Inc., Dallas, TX, USA) for 15 min and further centrifuged at 14,000 *g* at 4 °C for 20 min. The protein concentration of supernatant was tested by spectrophotometer (Thermo Fisher Scientific, Waltham, MA, USA). Same amount of protein samples were separated on 10%–12% SDS-PAGE gel by electrophoresis and then transferred onto nitrocellulose membranes (0.2 μm). Subsequently, the whole membranes were blocked with 5% non-fat blocking milk in Tris-buffered saline with 0.1% Tween 20 (1706531, Bio-Rad, Hercules, CA, USA) and incubated in primary antibodies overnight: rabbit anti-FGF21 (1:1000), rabbit anti-FGFR1 (1:2000), rabbit anti-FGFR1 (Phospho Y654, 1:2000), rabbit anti-PI3K (1:2000, 4292S, Cell Signaling Technology, Danvers, MA, USA), rabbit anti-Caspase-3 (1:1000, ab90437, Abcam, Cambridge, MA, USA), rabbit anti-cleaved Caspase-3 (1:1000, 9661S, Cell Signaling Technology, Danvers, MA, USA), rabbit anti-B-cell lymphoma 2 (anti-Bcl-2, 1:3000, sc-494, Santa Cruz Biotechnology Inc., Dallas, TX, USA), and mouse anti-Bcl-2-associated X protein (anti-Bax, 1:500, NBP1-28566, Novus Biologicals, Littleton, CO, USA). Mouse anti-β-actin (1:3000, Santa Cruz Biotechnology Inc., Dallas, TX, USA) as loading control. Next day, membranes were incubated in corresponding secondary antibodies (Santa Cruz Biotechnology Inc., Dallas, TX, USA) for 1 h at room temperature. Immunoblots were probed by the ECL plus kit (RPN2232, Amersham Bioscience, Arlington Heights, IL, USA). Blot bands were quantified by densitometry with ImageJ software and then were shown as relative density to β-actin.

2.13. Statistical analysis

All dates were analyzed with GraphPad Prism 7 (GraphPad Software, San Diego, CA, USA) and was expressed as mean ± standard

deviation (SD). Statistical difference between groups were analyzed with one-way or two-way analysis of variance (ANOVA) followed by multiple comparisons (Tukey or Sidak test). In addition, survival curve was analyzed with Log-rank (Mantel-Cox) test. Death toll and hemorrhage toll was analyzed with Fisher's exact test. p value $< .05$ was defined as statistical significance.

3. Results

3.1. Animal mortality and intracerebral hemorrhage

In total, 148 rats were used to establish MCAO models (did not include the cohort of intracerebroventricular injection of FGFR1 siRNA or scrambled siRNA GFP lentivirus), and 44 rats died within 3 d after surgery. After neurological score test, the 104 survival rats were randomly divided into two groups, pMCAO and rMCAO. Nine rats in pMCAO group and nine rats in rMCAO group died in the following study respectively. The overall mortality after MCAO/recanalization is 41.9% (Fig. 1 A). No significant difference in animal mortality was observed between pMCAO group (17.0%) and rMCAO group (17.6%) ($p > .05$, Fig. 1 A–C). The results showed recanalization did not significantly increase the animal mortality after MCAO. Fifty rats were pretreated with FGFR1 siRNA or scrambled siRNA GFP lentivirus via intracerebroventricular injection, and 15 rats died within 3 d after injection. Two rats in Scr siRNA group and three rats in FGFR1 siRNA group died in the following studies. No rats died in sham group (36 rats).

Intracerebral hemorrhage was identified by visible hemorrhagic spots and/or hemosiderin deposits on brain slices (Fig. 1 E). Due to an increased risk of hemorrhage by intracerebroventricular injection, rats pretreated with FGFR1 siRNA or scrambled siRNA GFP lentivirus were not analyzed together. Of the 44 rats that died within 3 d after MCAO, 10 rats occurred intracerebral hemorrhage, and 8 rats in pMCAO group and 7 rats in rMCAO group occurred intracerebral hemorrhage. The overall intracerebral hemorrhage rate after MCAO/recanalization was 16.9%, and no significant difference was observed between pMCAO group (15.1%) and rMCAO group (13.7%) ($p > .05$, Fig. 1 D–F). Therefore, the results suggested recanalization did not increase the intracerebral hemorrhage rate after MCAO in this study. No rats occurred intracerebral hemorrhage in sham group.

3.2. Serum FGF21 increased after MCAO/recanalization

Blood samples were collected from the heart of naïve rats and experimental rats at 3 d, 4 d, 10 d, and 30 d after MCAO. ELISA was performed to test the serum levels of FGF21. Serum FGF21 significantly increased at 3 d, 4 d, and 10 d after MCAO, peaked at 4 d ($p < .05$, Fig. 2 A). No significant difference was observed between pMCAO group and rMCAO group with respect to serum FGF21. Compared to pMCAO group, recanalization following MCAO did not change the serum levels of FGF21.

3.3. The expression of endogenous FGF21 and phosphorylated FGFR1 (p-FGFR1) in penumbra after MCAO/recanalization

The endogenous expression of FGF21 and p-FGFR1 in penumbra were evaluated at 3 d, 4 d, 10 d, and 30 d after MCAO. Compared to sham group, the level of FGF21 and p-FGFR1 increased significantly at 4 d and 10 d after MCAO (i.e. 1 d and 7 d after recanalization) in rMCAO group, and peaked at 4 d ($p < .05$, Fig. 2 B–C, E). However, the level of FGF21 and p-FGFR1 did not synchronously increased in pMCAO group. In the contralateral hemisphere (with no MCAO) of the pMCAO and rMCAO groups, FGF21 and p-FGFR1 expressions synchronously increased at 4 d and 10 d after MCAO, with no statistic difference between two groups (Fig. 2 A, D). These results suggested that MCAO significantly inhibited the expression of FGF21 and p-FGFR1 in ipsilateral penumbra. Recanalization abolished the inhibition and increased the expression of FGF21 and p-FGFR1 in penumbra after MCAO.

3.4. Recanalization increased the expression of endogenous FGF21 and p-FGFR1 in neurons at 4 d after MCAO

Double immunofluorescence staining of FGF21 and p-FGFR1 with NeuN was performed to evaluate the expression of FGF21 and p-FGFR1 in neurons in penumbra at 4 d after MCAO (i.e. 1 d after recanalization). Brain coronal slices were obtained at 4 d after MCAO. No statistic difference was observed between sham group and pMCAO group with respect to the expression of FGF21 and p-FGFR1 in neurons in penumbra. However, the number of FGF21-positive neuron and p-FGFR1-positive neuron significantly increased in penumbra in rMCAO group, compared to sham and pMCAO groups ($p < .05$, Fig. 3 A–E). These results showed that recanalization increased the expression of endogenous FGF21 and p-FGFR1 in neurons in penumbra at 4 d after MCAO (i.e. 1 d after recanalization).

3.5. Recanalization reduced infarct volume and improved neurological outcomes after MCAO

The TTC and Nissl staining were used only to calculate infarct volume in this study. Infarct volume and neurological deficits were tested at different timepoint after MCAO/recanalization. Compared to pMCAO group, recanalization reduced infarct volume and increased modified Garcia scores at 10 d and 30 d after MCAO in rMCAO group ($p < .05$, Fig. 4 A–D), however, no significant difference was observed between pMCAO group and rMCAO group at 4 d after MCAO (i.e. 1 d after recanalization). In beam walking test, a significant difference was observed between pMCAO group and rMCAO group at 10 d after MCAO, while no statistic difference was observed between two groups at 4 d and 30 d after MCAO ($p < .05$, Fig. 4 E).

Morris water maze was tested at 30 d after MCAO to evaluate the substantial spatial memory function of rats. Compared to sham group, rats in pMCAO group showed poor performance in terms of swimming distance, escape latency, and target quadrant time. Following recanalization, the swimming distance and escape latency significantly decreased in block 4 and 5, and the target quadrant time significantly increased ($p < .05$, Fig. 4 F–I). These results indicated that delayed-recanalization improved memory function at 30 d after MCAO.

3.6. Recanalization attenuated neuronal apoptosis after MCAO

TUNEL and FJC staining were performed to evaluate the neuronal apoptosis after MCAO/recanalization. Brain coronal slices were obtained at 4 d after MCAO (i.e. 1 d after recanalization). Compared to sham group, the number of TUNEL- and FJC-positive neuron significantly increased in pMCAO group, and recanalization after MCAO reduced the number of TUNEL- and FJC-positive neuron. Statistic difference was observed between pMCAO group and rMCAO group ($p < .05$, Fig. 5 A–E). The results showed that recanalization attenuated neuronal apoptosis at 4 d after MCAO

3.7. FGFR1 siRNA weakened the effects of recanalization on neurological outcomes at 10 d after MCAO

To investigate the potential molecular mechanism of the FGF21 anti-apoptosis effect, intracerebroventricular injection of FGFR1 siRNA GFP lentivirus was performed at 1 h before MCAO to knockdown FGFR1 expression in neurons. Brain coronal slices were obtained at 4 d after intracerebroventricular injection and stained with DAPI and/or NeuN. Fluorescence microphotographs showed FGFR1 siRNA lentivirus successfully transduced neurons (Fig. 6 A–B).

After recanalization, the infarct volume was reduced, and modified

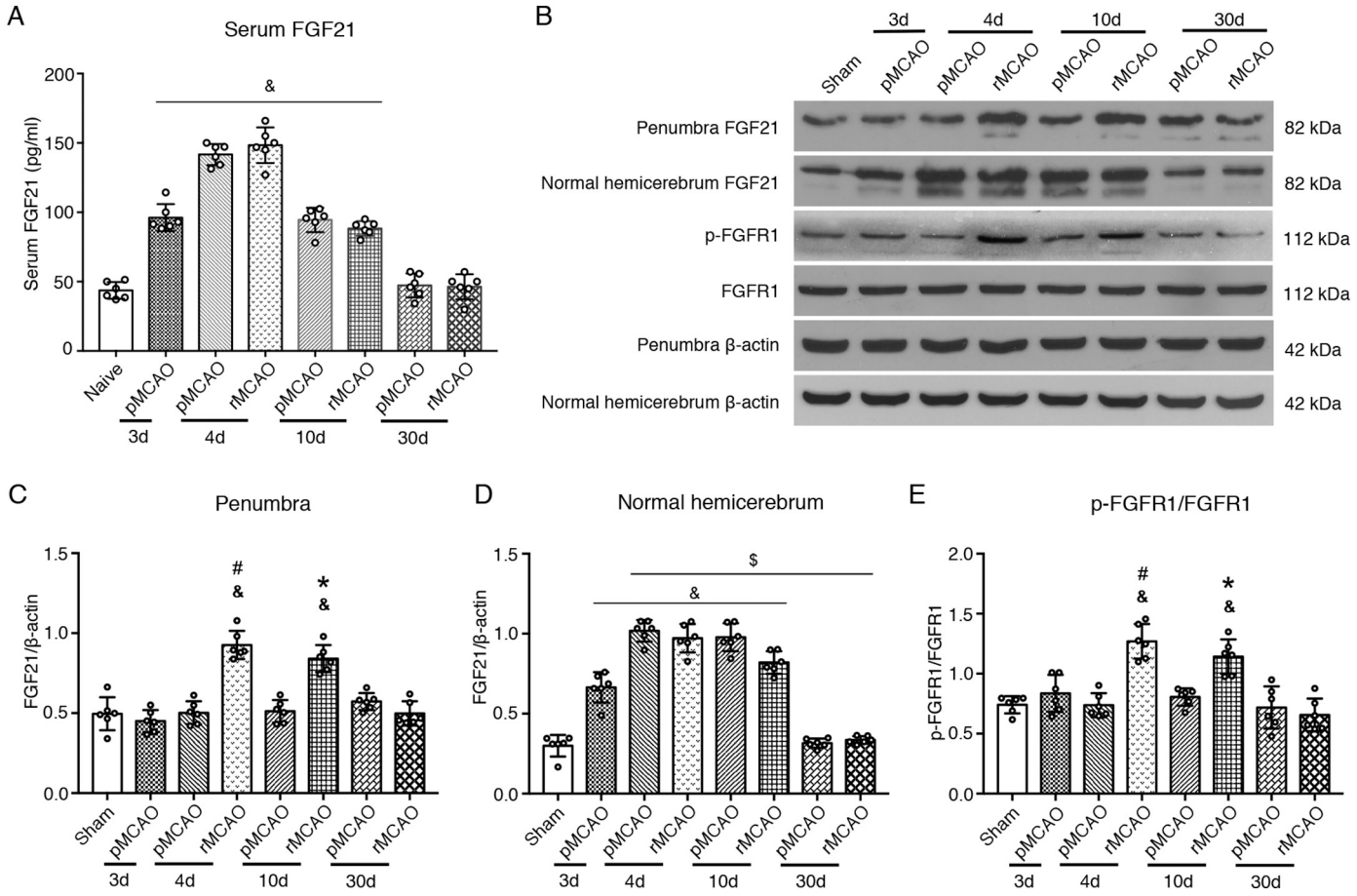

Fig. 2. The expression of serum FGF21, cerebral FGF21 and FGFR1 after MCAO/recanalization. (A) Quantitative analyses of serum FGF21; (B) Representative Western blots images; (C–E) Quantitative analyses of cerebral FGF21 and p-FGFR1, $^{\&}p < .05$, vs sham, $^{\$}p < .05$, vs pMCAO 3d, $^{\#}p < .05$, vs pMCAO 4d, $^{*}p < .05$, vs pMCAO 10d, n = 6 per group, One-way ANOVA-Tukey. FGF21, fibroblast growth factor 21; FGFR1, fibroblast growth factor receptor 1; p-FGFR1, phosphorylated FGFR1; pMCAO, permanent middle cerebral artery occlusion; rMCAO, recanalization at 3 d after MCAO; d, day.

Garcia scores and beam walking scores were increased in rMCAO group at 10 d after MCAO, compared to pMCAO group. However, with administration of FGFR1 siRNA, the infarct volume significantly was increased, modified Garcia scores and beam walking scores were significantly decreased in FGFR1 siRNA group, compared to rMCAO and Scr siRNA groups ($p < .05$, Fig. 6 D–G). In addition, modified Garcia scores showed statistic difference between pMCAO group and FGFR1 siRNA group. These results indicated that pretreatment of FGFR1 siRNA weakened the effects of recanalization on neurological outcomes at 10 d after MCAO.

3.8. FGF21 attenuated neuronal apoptosis through FGFR1/PI3K/Caspase-3 signaling pathway at 4 d after MCAO

To investigate the potential molecular mechanism of the FGF21 anti-apoptosis effect, intracerebroventricular injections of FGFR1 siRNA GFP lentivirus or scrambled siRNA GFP lentivirus were performed at 1 h before MCAO to knockdown FGFR1 expression on neurons. Recanalization was performed at 3 d after MCAO. Western blots were performed at 4 d after MCAO. The results of Western blot showed that Bcl-2 significantly decreased, and CC3 and Bax increased after MCAO in penumbra compared with sham group ($p < .05$, Fig. 7 A, F–H). At the same time, there is no statistic difference between pMCAO group and sham group with respect to the expression of FGF21, p-FGFR1, FGFR1, and PI3K ($p > .05$, Fig. 7 A–E). Following recanalization in rMCAO group, the expression FGF21, p-FGFR1, PI3K, and Bcl-2 significantly increased, CC3 and Bax expression decreased, compared with pMCAO group ($p < .05$, Fig. 7 A–H). No statistic differences were observed between rMCAO group and Scr siRNA group with respect to the expressions of FGF21, p-FGFR1, FGFR1, PI3K, Bcl-2, CC3 and Bax. While following pretreatment of FGFR1 siRNA, the expressions of p-FGFR1, PI3K, and Bcl-2 significantly decreased associated with the silencing of FGFR1 expression, reversely, CC3 and Bax increased in FGFR1 siRNA group, compared with rMCAO group ($p < .05$, Fig. 7 C–H). The results showed that FGFR1 siRNA inhibited the FGFR1 expression, decreased the PI3K expression, and abolished the anti-apoptosis effect of FGF21.

4. Discussion

A main treating goal of acute ischemic stroke is to restore the cerebral blood flow (Savitz et al., 2017). Previous guidelines recommended that endovascular thrombectomy should be initiated within 6 h in patients with occlusion of ICA or the first segment of MCA (Albers et al., 2018). Multiple evidences showed that reperfusion exceeded 6 h induced ischemia/reperfusion injury, increased hemorrhagic transformation, and deteriorated neurological outcomes in animal models (McBride and Zhang, 2017). While, an increasing number of clinical evidences showed that delayed recanalization (thrombectomy and spontaneous recanalization exceeded 6 h) salvaged ischemic tissue and improved neurological outcomes in ischemic stroke patients (Nogueira et al., 2018; Albers et al., 2018; Jovin et al., 2011; Lansberg et al., 2015; Jiang et al., 2019). The updated guideline from the American Heart Association/American Stroke Association (AHA/ASA) also recommends to perform mechanical thrombectomy in selected LVO

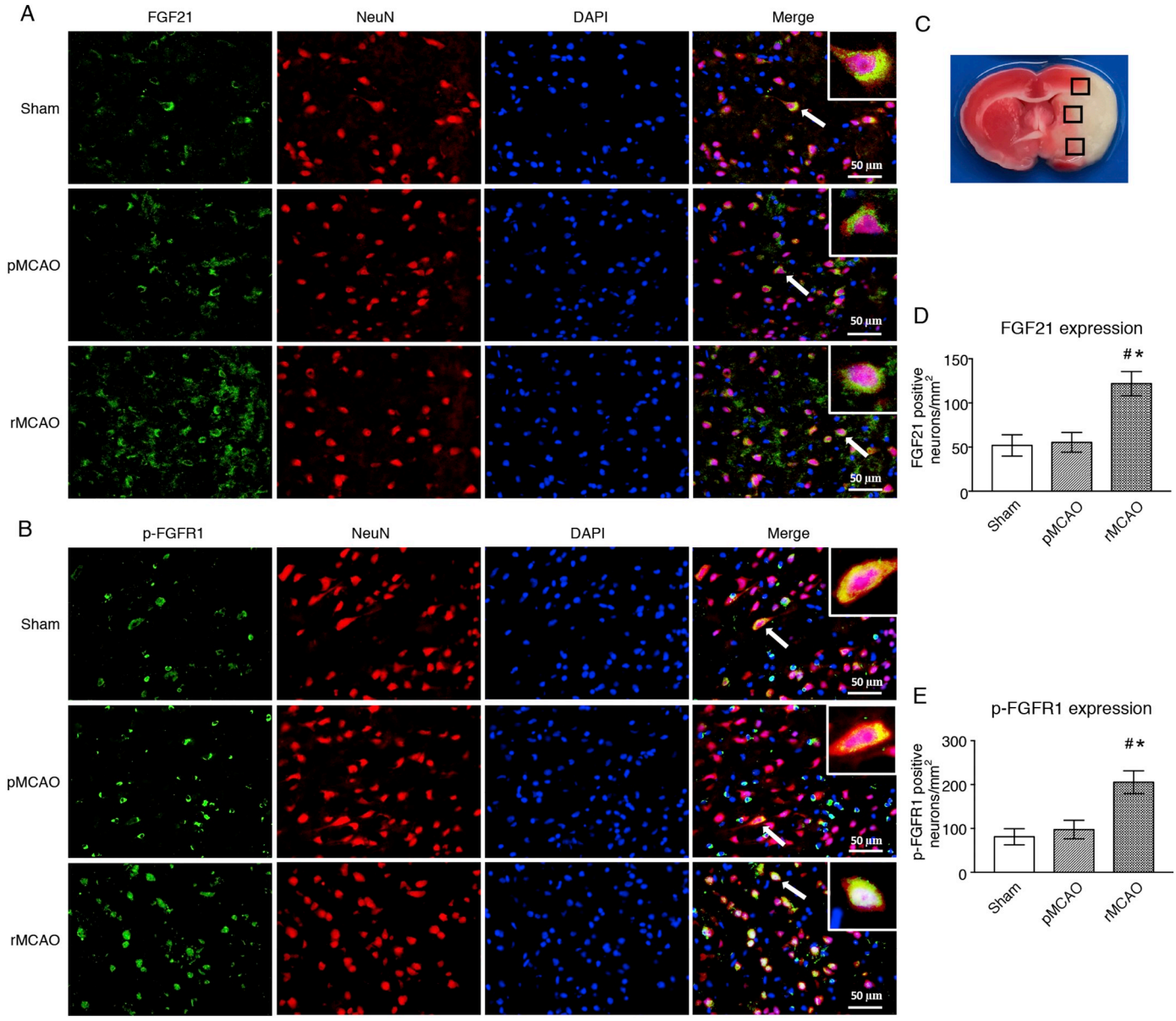

Fig. 3. Recanalization increased the expression of FGF21 and p-FGFR1 in neurons at 4 d after MCAO. (A–B) Representative microphotographs of FGF21 and p-FGFR1 (Green) colocalized with neurons (NeuN, Red). DAPI (Blue) marked Nuclei, Scale bar = 50 μm; (C) Samples were obtained from ischemic penumbra; (D–E) Quantitative analyses of FGF21- and p-FGFR1-positive neurons, $^{\#}p < .05$, vs sham, $^{*}p < .05$, vs pMCAO, n = 3 (3 sections per slice), One-way ANOVA-Tukey. pMCAO, permanent middle cerebral artery occlusion; rMCAO, recanalization at 3 d after MCAO; FGF21, fibroblast growth factor 21; p-FGFR1, phosphorylated fibroblast growth factor receptor 1; NeuN, neuronal nuclei; DAPI, 4′,6-diamidino-2-phenylindole. (For interpretation of the references to colour in this figure legend, the reader is referred to the web version of this article.)

patients up to 16 h or 24 h after symptom onset, following evaluating by computed tomographic perfusion, diffusion-weighted MRI, or MRI perfusion (Kelly and Holloway, 2018). Therefore, it was revealed that delayed recanalization did not induce serious ischemia/reperfusion injury in a part of selected LVO patients. The underlying molecular mechanisms remain mystery.

In this study, we investigated the neurological outcomes after delayed recanalization in pMCAO rats and the potential roles of endogenous neuroprotective agent FGF21 in neuronal anti-apoptosis after ischemia/reperfusion. We demonstrated that delayed recanalization at 3 d after MCAO decreased infarct volume and improved neurobehavioral deficits, with no increasing of animal mortality rate and intracerebral hemorrhage rate. Meanwhile, we found endogenous neuroprotective agent FGF21 significantly increased in serum after MCAO. Furthermore, we observed that FGF21 and p-FGFR1 robustly expressed on neurons in penumbra in a time-dependent manner after recanalization in rMCAO rats, while which did not increase in penumbra in pMCAO rats. At last, we certified that FGF21 and p-FGFR1 activated PI3K/Caspase-3 signaling pathway to attenuate neuronal apoptosis in penumbra after recanalization. Conversely, knockdown of FGFR1 using FGFR1 siRNA abolished the anti-apoptotic effects of FGF21, and in part abrogated beneficial effects of recanalization on neurological outcomes.

Although the clinical evidence for reperfusion injury is less clear in stroke patient (Savitz et al., 2017), previous evidences supported that recanalization exceeded the time window might enhance brain edema and induce ischemia/reperfusion injury in ischemic animal models (Kneihsl et al., 2018; Hao et al., 2017; Yaghi et al., 2014), which may increase the animal mortality. Additionally, the subsequent reactive hyperemia/hyperperfusion and damage of cerebral blood vessels, especially in infarct lesions, might be related to intracerebral

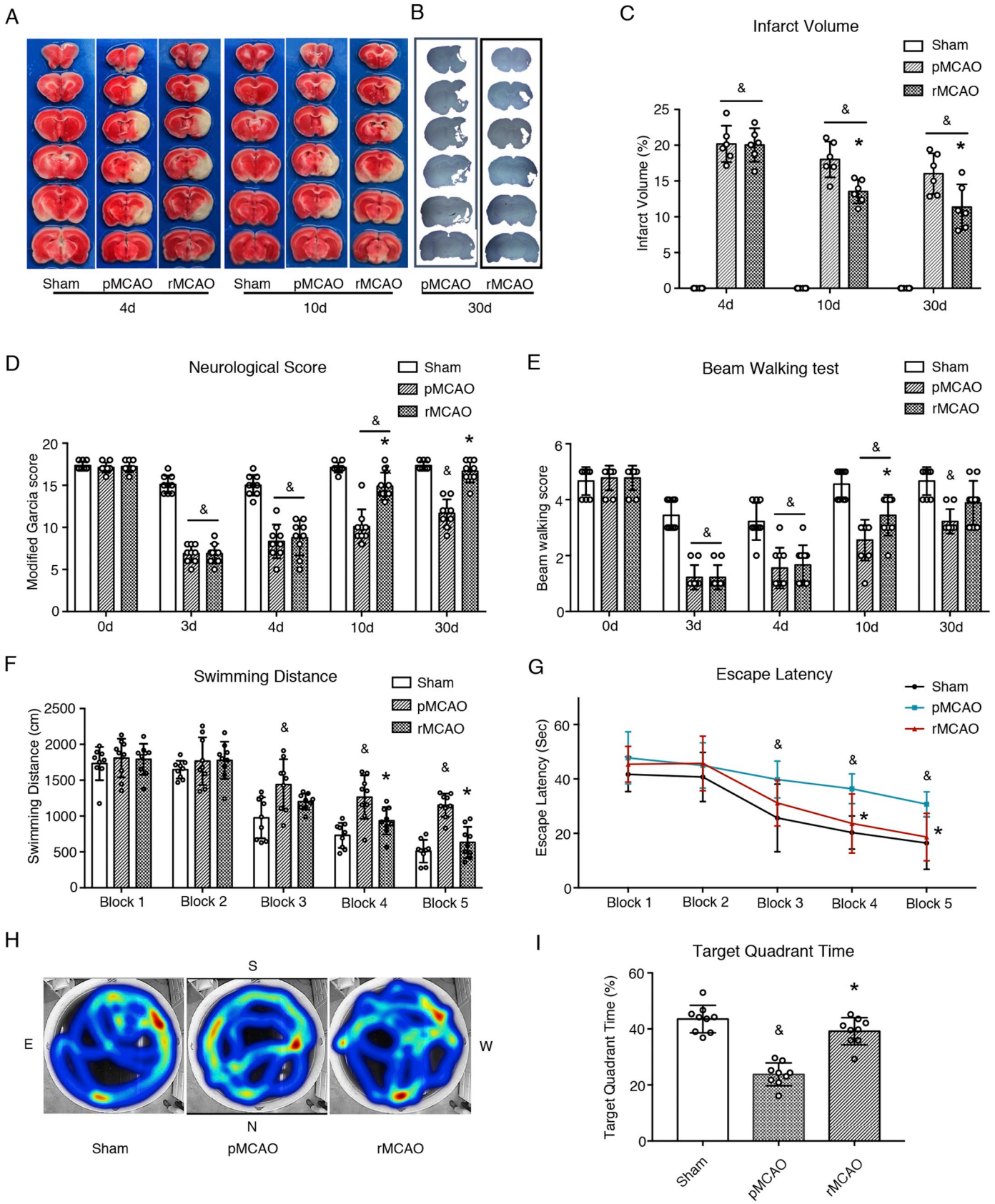

Fig. 4. Recanalization reduced infarct volume and improved neurological outcomes after MCAO. TTC and Nissl staining were only used to calculate infarct volume. (A) Representative images of TTC stained brain slices; (B) Representative images of Nissl stained brain slices. (C) Quantified infarct volume, (D) Modified Garcia score, (E) Beam walking score, (F) Swimming distance, and (G) Escape latency, $^{\&}p < .05$, vs sham, $^{*}p < .05$, vs pMCAO, n = 9 per group, Two-way ANOVA-Sidak; (H) Heatmap image; (I) Target quadrant time, $^{\&}p < .05$, vs sham, $^{*}p < .05$, vs pMCAO, n = 9 per group, One-way ANOVA-Tukey. pMCAO, permanent middle cerebral artery occlusion; rMCAO, recanalization at 3 d after MCAO; d, day.

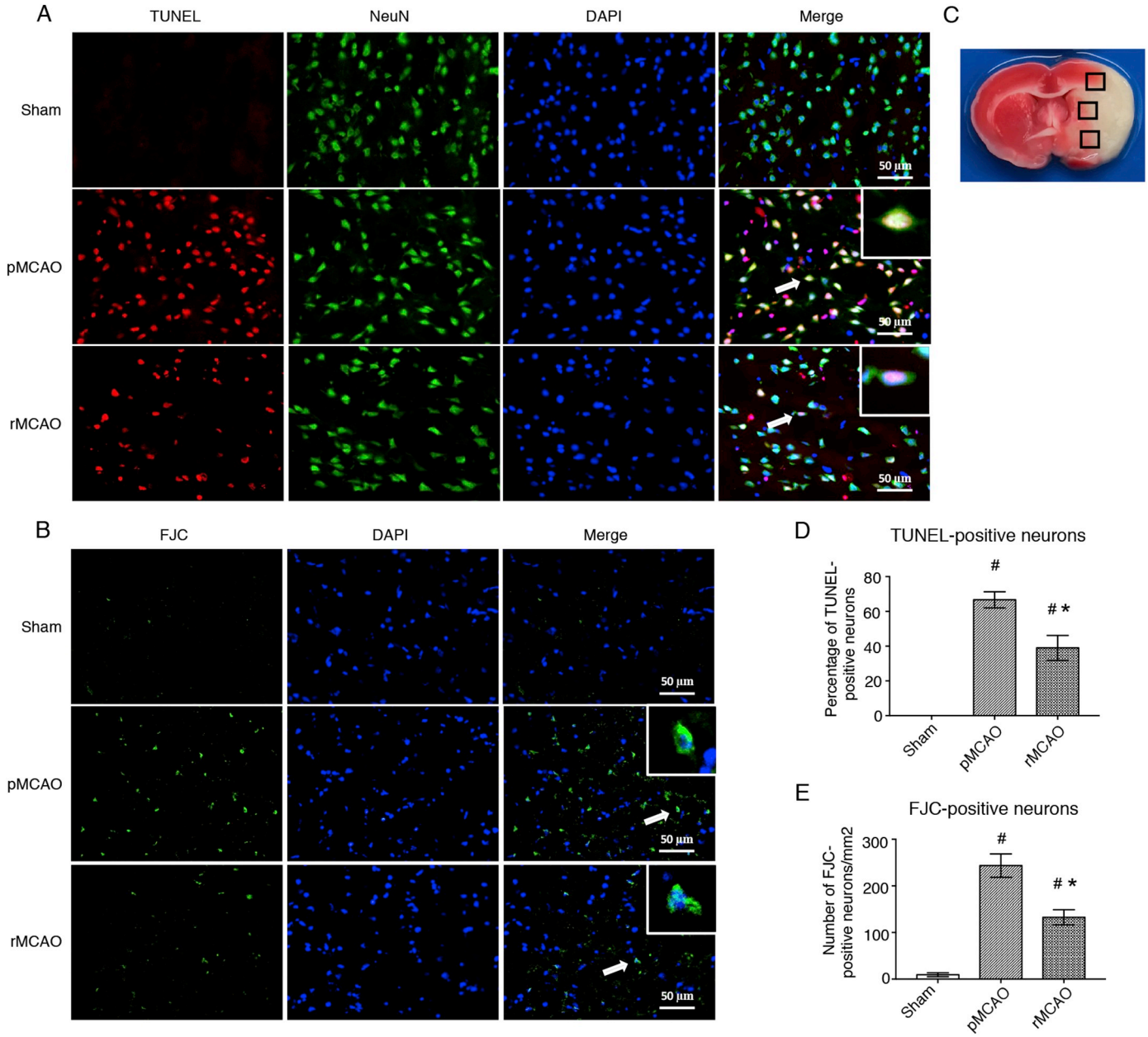

Fig. 5. Recanalization reduced neuronal apoptosis at 4 d after MCAO. (A) Representative microphotographs of TUNEL staining positive (Red) neurons (NeuN, Green). (B) Representative microphotographs of FJC staining positive (Green) neurons. DAPI (Blue) marked Nuclei. Scale bar = 50 μm. (C) Samples obtained from ischemic penumbra (three sections per slice). (D) Quantitative analyses of TUNEL-positive neurons, (E) Quantitative analyses of FJC-positive neurons, $^{\#}p < .05$, vs sham, $^{*}p < .05$, vs pMCAO, n = 3 (3 sections per slice), One-way ANOVA-Tukey. pMCAO, permanent middle cerebral artery occlusion; rMCAO, recanalization at 3 d after MCAO; TUNEL, Terminal deoxynucleotidyl transferase dUTP nick end labeling (staining); FJC, Fluoro-Jade (staining); NeuN, neuronal nuclei; DAPI, 4′,6-diamidino-2-phenylindole. (For interpretation of the references to colour in this figure legend, the reader is referred to the web version of this article.)

hemorrhage (Kneihsl et al., 2018). Our previous study demonstrated that delayed recanalization restored cerebral blood flow in penumbra after MCAO (McBride et al., 2018). In present study, we found that delayed recanalization reduced infarct volume and increased the modified Garcia score at 10 d and 30 d after MCAO, increased beam walking score at 10 d after MCAO, and improved the performances in Morris Water Maze at 30 d after MCAO, compared to pMCAO group. In addition, no significant differences were observed between two groups with respect to the animal mortality rate (17.0% in pMCAO group vs 17.6% in rMCAO group) and intracerebral hemorrhage rate (15.1% in pMCAO group vs 13.7% in rMCAO group), although the higher mortality rate (29.7%) and higher intracerebral hemorrhage rate (22.7%) were observed within 3 d after MCAO (before rats grouped and recanalization). These results suggested delayed recanalization improved neurological outcomes after MCAO, with no increasing animal mortality and intracerebral hemorrhage.

Our findings accorded with several other results in different studies. A previous evidence revealed that delayed recanalization via mechanical thrombectomy at 20 h after MCAO did not increased the hemorrhagic transformation and infarct size in young adult baboons (Giffard et al., 2005). Recently, a clinical trial involved 206 ischemic stroke patients demonstrated that thrombectomy at 6–24 h after stroke onset did not increase the symptomatic intracranial hemorrhage rate (6% in thrombectomy group vs 3% in control group) and 90-day mortality rate (19% vs 18%, respectively), compared to control group (Nogueira et al., 2018). According with another update clinical trial, two studies showed

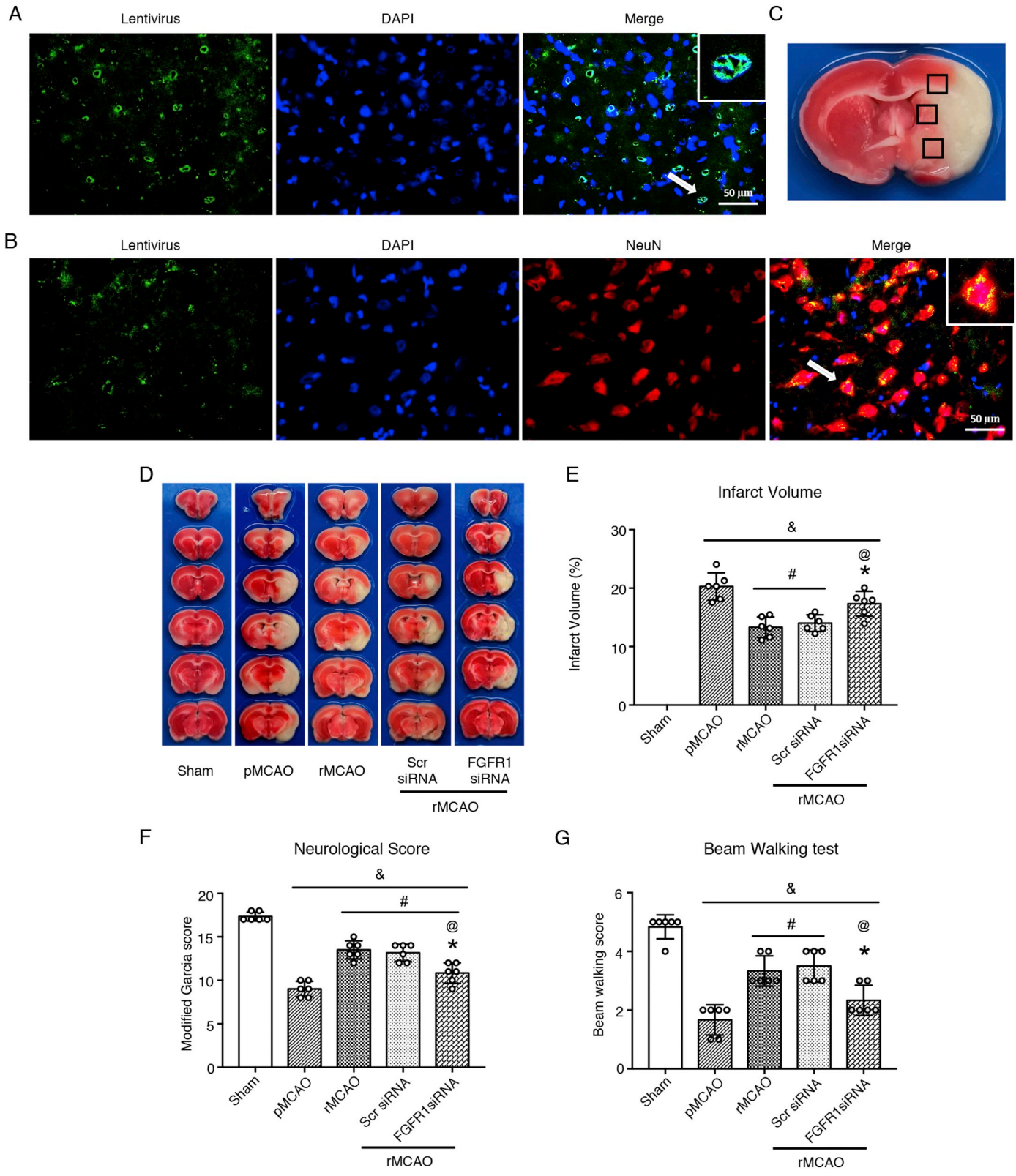

Fig. 6. FGFR1 siRNA weakened the effects of recanalization on neurological outcome at 10 d after MCAO. (A–B) Representative microphotographs of FGFR1 siRNA lentivirus (GFP, Green) transduced neurons (NeuN, Red) at 4 d after intracerebroventricular injection, A was observed after rat sacrifice at once, B was observed at 24 h after sacrifice with NeuN staining. DAPI (Blue) marked Nuclei. Scale bar = 50 μm. (C) Samples were obtained from the ischemic penumbra. (D) Representative images of TTC stained brain slices. TTC staining was only used to calculate infarct volume; (E) Quantified infarct volume; (F) Modified Garcia score, and (G) Beam walking score, $^{\&}p < .05$, vs sham, $^{\#}p < .05$, vs pMCAO, $^{*}p < .05$, vs rMCAO, $^{@}p < .05$, vs Scr siRNA, n = 6 per group, One-way ANOVA-Tukey. NeuN, neuronal nuclei; DAPI, 4′,6-diamidino-2-phenylindole; pMCAO, permanent middle cerebral artery occlusion; rMCAO, recanalization at 3 d after MCAO; Scr siRNA, scrambled siRNA; FGFR1, fibroblast growth factor receptor 1. (For interpretation of the references to colour in this figure legend, the reader is referred to the web version of this article.)

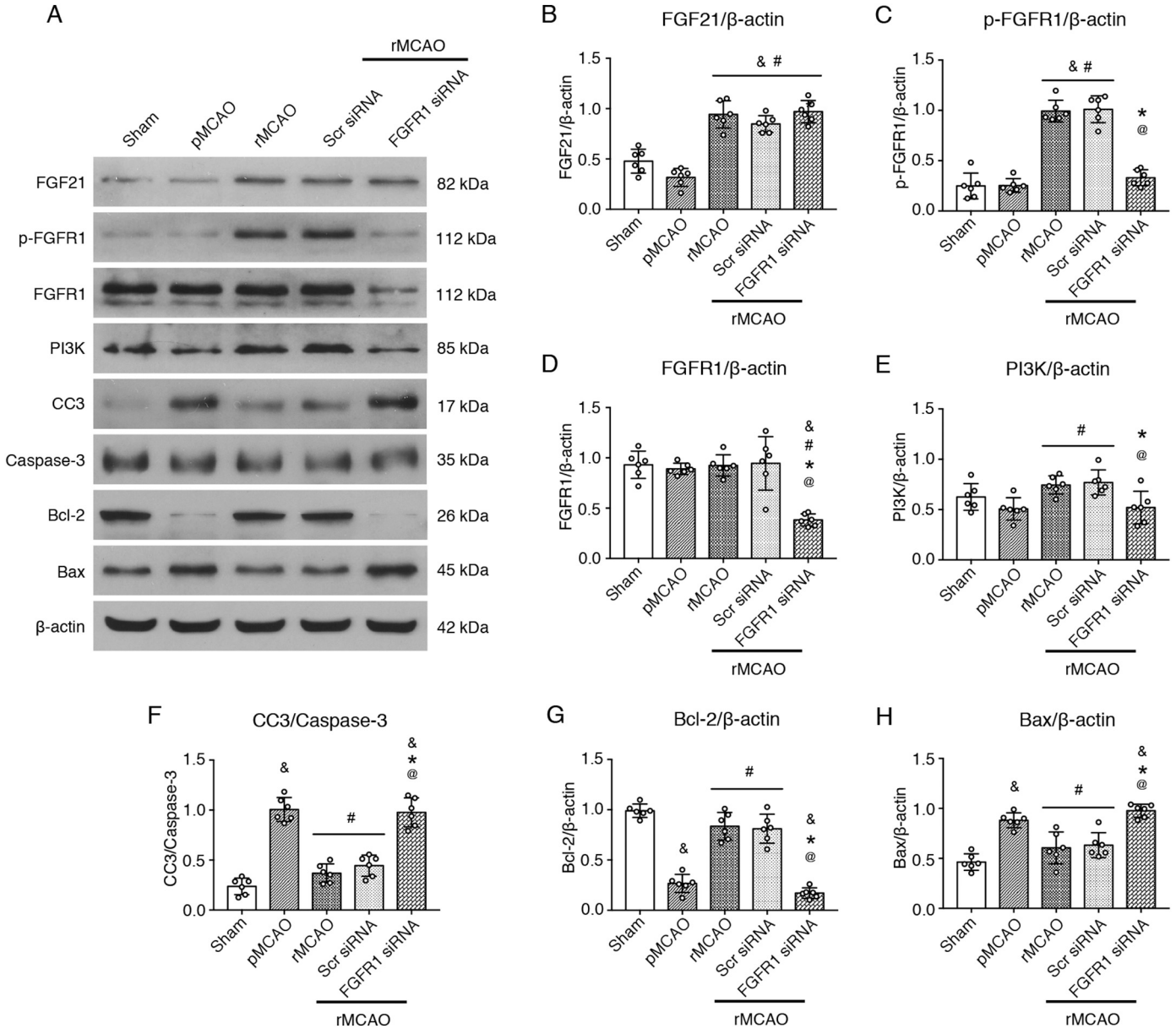

Fig. 7. Effects of FGF21 on neuronal apoptosis via FGFR1/PI3K/Caspase-3 signaling pathway at 1 d after recanalization. (A) Representative Western blots images; (B–H) Quantitative analyses of FGF21, p-FGFR1, FGFR1, PI3K, CC3, Bcl-2, and Bax, $^{\&}p < .05$, vs sham, $^{\#}p < .05$, vs pMCAO, $^{*}p < .05$, vs rMCAO, $^{@}p < .05$, vs Scr siRNA, n = 6 per group, One-way ANOVA-Tukey. pMCAO, permanent middle cerebral artery occlusion; rMCAO, recanalization at 3 d after MCAO; Scr siRNA, scrambled siRNA; FGF21, fibroblast growth factor 21; FGFR1, fibroblast growth factor receptor 1; p-FGFR1, phosphorylated FGFR1; PI3K, phosphatidylinositol-4,5-bisphosphate 3-kinase; CC3, cleaved Caspase-3; Bcl-2, B-cell lymphoma 2; Bax, Bcl-2-associated X protein.

that recanalization within 6–24 h after stroke remarkably improved 90-day clinical outcomes in patients with salvageable hypoperfusion tissue after LVO (Albers et al., 2018; Nogueira et al., 2018).

The interesting findings in our study obviously varied from multiple evidences at the experimental level that ischemia/reperfusion injury triggered by delayed recanalization might deteriorate outcomes after MCAO (Savitz et al., 2017; Aronowski et al., 1997). The underlying fact is the selected survival rats (modified Garcia score ranging from 6 to 9) with moderate size of ischemic core and a substantial amount of penumbra, compared to the rats with lower score or died within 3 d after MCAO, as well as the patients with salvageable hypoperfusion tissue before thrombectomy. Delayed recanalization may salvage the extensive ischemic tissue at risk of infarction, which may improve neurological outcomes.

Several lines of studies observed that various endogenous neuroprotective agents contribute to reducing oxidative stress, decreasing glutamate release, sustaining intracellular Ca^{2+} levels, preventing mitochondrial collapse, protecting blood-brain barrier, and inhibiting neuroinflammation in stroke models (Kim et al., 2018; Pena et al., 2017; Reis et al., 2017; Savitz et al., 2017). FGF21 is a multifunctional metabolic stress-inducible hormone and is robustly expressed in liver under normal conditions (Salminen et al., 2017b), with a low expression level in human brain, thymus, and pancreas (Staiger et al., 2017). Under certain physiological and pathological cellular/organelle stress, e.g. mitochondrial or endoplasmic reticulum (ER) stress, may activate the PERK/eIF2α/ATF4 axis and induce FGF21 secreting remarkably from several extrahepatic tissues (Salminen et al., 2017b), such as adipose tissue, pancreas, kidney, skeletal muscles, and cardiac muscles, as well as liver (Luo et al., 2017; Salminen et al., 2017a; Liu et al., 2013; Salminen et al., 2017b). The upregulated serum FGF21 may directly target relevant organs, e.g. heart and liver, to attenuate tissue stresses and promote tissue survival by interacting with FGFR1 to activate

downstream signaling pathways (Salminen et al., 2017b; Staiger et al., 2017; Liu et al., 2013). In addition, the increased FGF21 may induce the secreting of adiponectin and corticosterone, which synchronously contribute to tissue survival in stresses (Salminen et al., 2017b). There are mounting evidences supported that serum FGF21 was significantly upregulated in different diseases and alleviated relevant tissue injury (Salminen et al., 2017a). A study indicated that serum FGF21 dramatically increased after ischemia/reperfusion injury in patients with liver transplantation (Ye et al., 2016). Congruently, following myocardial ischemia/reperfusion injury in the mouse, serum endogenous FGF21 observably secreted from several tissues and phosphorylated FGFR1 in cardiomyocytes, which activated PI3K/serine-threonine kinase (Akt)/Bcl-2 associated agonist of cell death (BAD) signaling cascade, subsequently reducing Caspase-3 activity and cell death (Liu et al., 2013). It was also reported that FGF21 obviously inhibited oxidative stress, inflammation, and apoptosis through Sirtuin-1 (SIRT1)/liver kinase B1 (LKB1)/AMP-activated protein kinase (AMPK) signaling pathway, ameliorating doxorubicin (DOX)-induced cardiotoxicity (Wang et al., 2017). In H9c2 cells, administration of exogenous FGF21 attenuated ischemia/reperfusion injury through activating Akt/glycogen synthase kinase 3β (GSK-3β)/Caspase-3 signaling pathway (Cong et al., 2013).

In murine and human brain, FGF21 is capable to pass the blood-brain barrier and expressed in neurons in different brain regions (Wang et al., 2016; Staiger et al., 2017). It was reported that lithium, valproate, and histone deacetylase (HDAC) inhibitors can upregulate FGF21 expression in brain (Salminen et al., 2017b). Injury in brain, e.g. cerebral ischemia/reperfusion injury, may trigger oxidative stress and activate the integrated stress response (ISR) pathway, which subsequently provoked neuronal apoptosis (Salminen et al., 2017b). The stress kinases of ISR pathway synchronously activated transcription factor ATF4, which may subsequently induce the secreting of FGF21 from several tissues (Salminen et al., 2017b). However, it was reported that FGF21 expression levels significantly decreased in ischemic cortex and striatum after MCAO, but FGF21 mRNA levels were not affected (Wang et al., 2016). In our study, although endogenous FGF21 significantly increased in serum after MCAO, we identified that FGF21 did not accordingly increase in penumbra in pMCAO group. However, the expression of FGF21 and p-FGFR1 robustly increased in penumbra following recanalization in rMCAO group. These results suggested that hypoperfusion after MCAO prevented serum FGF21 expressing in ischemic area. Reversely, recanalization restored the cerebral blood flow and enhanced FGF21 levels in penumbra.

As a neuroprotective agent, it was certified that FGF21 can attenuate cell apoptosis, oxidative stress, mitochondrial energy metabolism disorder, and excitotoxicity to combat tissue injury in multiple neurological diseases via activation of downstream signaling pathways, including AMPK, mitogen-activated protein kinases (MAPK)/extracellular signal-related kinases (ERK), and PI3K/Akt signaling cascades (Salminen et al., 2017a; Sa-Nguanmoo et al., 2016; Salminen et al., 2017b; Wang et al., 2016). Moreover, FGF21 may activate somatotropic axis and hypothalamic-pituitary-adrenal (HPA) axis in response to various stresses (Salminen et al., 2017a; Salminen et al., 2017b). In our study, double immunofluorescence staining showed that FGF21 and p-FGFR1 robustly expressed on neurons in penumbra. In consideration of the provoked neuronal apoptosis after ischemic stroke and the anti-apoptosis effects of FGF21 in hepatic and myocardial ischemia/reperfusion injury (Savitz et al., 2017; Ye et al., 2016; Liu et al., 2013), we mainly focused on the neuronal apoptosis after MCAO and recanalization. In present study, the TUNEL staining and FJC staining showed that ischemia following MCAO significantly provoked neuronal apoptosis in penumbra, as same as previous evidences (Yu et al., 2018). While recanalization at 3 d after MCAO dramatically attenuated neuronal apoptosis as showed by TUNEL and FJC staining. Western blot also indicated the apoptosis marker Bcl-2 expression increased and Bax expression decreased following recanalization, compared to pMCAO. At the same time, we found the expression of p-FGFR1 and PI3K increased, and the activation of Caspase-3 decreased in penumbra as seen from Western blot results, corresponding to the increase of FGF21 expression. After pretreatment of FGFR1 siRNA, our results revealed that knocking down of FGFR1 abolished the anti-apoptotic effects of FGF21 as seen from the expression of PI3K, cleaved Caspase-3, Bcl-2, and Bax, which partly reversed the beneficial effects of recanalization on neurological outcomes after MCAO (the infarct volume increased, modified Garcia scores and beam walking scores decreased, compared to rMCAO group). The findings suggested that the increase of FGF21 following recanalization attenuated neuronal apoptosis in penumbra via FGFR1/PI3K/Caspase-3 signaling pathway, at least in part, which improved the neurological outcomes in pMCAO rats.

In conclusion, the present study firstly demonstrated that delayed recanalization at 3 d after MCAO enhanced endogenous neuroprotective agent FGF21 expression in penumbra, which contributed to attenuating neuronal apoptosis in penumbra though FGFR1/PI3K/Caspase-3 signaling pathway, and at least in part, improving the neurobehavior functions in MCAO rats. Furthermore, delayed recanalization at 3 d after MCAO did not increase the animal mortality and intracerebral hemorrhage rate in experimental rats. Basing on our findings and the clinical evidences of spontaneous recanalization, delayed recanalization that exceeds 24 h or more long time may be a promising treatment strategy in selected ischemic stroke patients, which merits further investigation.

Acknowledgement

None.

Funding

This work was partially supported by the National Institutes of Health [grant numbers: NS081740 and NS082184]

Author contributions

JHZ, JT, and WZ developed the concept of this study; WZ and NM designed this study. WZ, JP, XL, and ZS acquired and analyzed data. JHZ, WZ, and NM drafted the manuscript and figures. All authors critically reviewed the manuscript and approved the final version to be published.

Declartion of Competing Interest

None.

References

Albers, G.W., Marks, M.P., Kemp, S., Christensen, S., Tsai, J.P., Ortega-Gutierrez, S., McTaggart, R.A., Torbey, M.T., Kim-Tenser, M., Leslie-Mazwi, T., Sarraj, A., Kasner, S.E., Ansari, S.A., Yeatts, S.D., Hamilton, S., Mlynash, M., Heit, J.J., Zaharchuk, G., Kim, S., Carrozzella, J., Palesch, Y.Y., Demchuk, A.M., Bammer, R., Lavori, P.W., Broderick, J.P., Lansberg, M.G., 2018. Thrombectomy for stroke at 6 to 16 hours with selection by perfusion imaging. N. Engl. J. Med. 378 (8), 708–718. https://doi.org/10.1056/NEJMoa1713973.

Aronowski, J., Strong, R., Grotta, J.C., 1997. Reperfusion injury: demonstration of brain damage produced by reperfusion after transient focal ischemia in rats. J. Cereb. Blood Flow Metab. 17 (10), 1048–1056. https://doi.org/10.1097/00004647-199710000-00006.

Chen, C.J., Ding, D., Starke, R.M., Mehndiratta, P., Crowley, R.W., Liu, K.C., Southerland, A.M., Worrall, B.B., 2015. Endovascular vs medical management of acute ischemic stroke. Neurology 85 (22), 1980–1990. https://doi.org/10.1212/WNL.0000000000002176.

Cloft, H.J., Rabinstein, A., Lanzino, G., Kallmes, D.F., 2009. Intra-arterial stroke therapy: an assessment of demand and available work force. AJNR Am. J. Neuroradiol. 30 (3), 453–458. https://doi.org/10.3174/ajnr.A1462.

Cong, W.T., Ling, J., Tian, H.S., Ling, R., Wang, Y., Huang, B.B., Zhao, T., Duan, Y.M., Jin, L.T., Li, X.K., 2013. Proteomic study on the protective mechanism of fibroblast growth factor 21 to ischemia-reperfusion injury. Can. J. Physiol. Pharmacol. 91 (11), 973–984. https://doi.org/10.1139/cjpp-2012-0441.

Garcia, J.H., Wagner, S., Liu, K.F., Hu, X.J., 1995. Neurological deficit and extent of

neuronal necrosis attributable to middle cerebral artery occlusion in rats. Statistical validation. Stroke 26 (4), 627–634 (635).
Giffard, C., Young, A.R., Mezenge, F., Derlon, J.M., Baron, J.C., 2005. Histopathological effects of delayed reperfusion after middle cerebral artery occlusion in the anesthetized baboon. Brain Res. Bull. 67 (4), 335–340. https://doi.org/10.1016/j.brainresbull.2005.08.001.
Goldstein, L.B., Davis, J.N., 1990. Beam-walking in rats: studies towards developing an animal model of functional recovery after brain injury. J. Neurosci. Methods 31 (2), 101–107.
Gonzalez, R.G., Furie, K.L., Goldmacher, G.V., Smith, W.S., Kamalian, S., Payabvash, S., Harris, G.J., Halpern, E.F., Koroshetz, W.J., Camargo, E.C., Dillon, W.P., Lev, M.H., 2013. Good outcome rate of 35% in IV-tPA-treated patients with computed tomography angiography confirmed severe anterior circulation occlusive stroke. Stroke 44 (11), 3109–3113. https://doi.org/10.1161/STROKEAHA.113.001938.
Gopalakrishnan, A., Shankarappa, S.A., Rajanikant, G.K., 2019. Hydrogel scaffolds: towards restitution of ischemic stroke-injured brain. Transl. Stroke Res. 10 (1), 1–18. https://doi.org/10.1007/s12975-018-0655-6.
Griemert, E.V., Recarte, P.K., Engelhard, K., Schafer, M.K., Thal, S.C., 2018. PAI-1 but not PAI-2 gene deficiency attenuates ischemic brain injury after experimental stroke. Transl. Stroke Res. https://doi.org/10.1007/s12975-018-0644-9.
Gubskiy, I.L., Namestnikova, D.D., Cherkashova, E.A., Chekhonin, V.P., Baklaushev, V.P., Gubsky, L.V., Yarygin, K.N., 2018. MRI guiding of the middle cerebral artery occlusion in rats aimed to improve stroke modeling. Transl. Stroke Res. 9 (4), 417–425. https://doi.org/10.1007/s12975-017-0590-y.
Hao, Y., Yang, D., Wang, H., Zi, W., Zhang, M., Geng, Y., Zhou, Z., Wang, W., Xu, H., Tian, X., Lv, P., Liu, Y., Xiong, Y., Liu, X., Xu, G., 2017. Predictors for symptomatic intracranial hemorrhage after endovascular treatment of acute ischemic stroke. Stroke 48 (5), 1203–1209. https://doi.org/10.1161/STROKEAHA.116.016368.
Jiang, W.J., Liu, A.F., Yu, W., Qiu, H.C., Zhang, Y.Q., Liu, F., Li, C., Wang, R., Zhao, Y.L., Lv, J., Li, T.X., Liu, C., Zhou, J., Zhao, J.Z., 2019. Outcomes of Multimodality in situ Recanalization in Hybrid Operating Room (MIRHOR) for symptomatic chronic internal carotid artery occlusions. J. Neurointerv. Surg. https://doi.org/10.1136/neurintsurg-2018-014384.
Jovin, T.G., Liebeskind, D.S., Gupta, R., Rymer, M., Rai, A., Zaidat, O.O., Abou-Chebl, A., Baxter, B., Levy, E.I., Barreto, A., Nogueira, R.G., 2011. Imaging-based endovascular therapy for acute ischemic stroke due to proximal intracranial anterior circulation occlusion treated beyond 8 hours from time last seen well: retrospective multicenter analysis of 237 consecutive patients. Stroke 42 (8), 2206–2211. https://doi.org/10.1161/STROKEAHA.110.604223.
Kelly, A.G., Holloway, R.G., 2018. Guideline: the AHA/ASA made 217 recommendations for early management of acute ischemic stroke in adults. Ann. Intern. Med. 168 (12), C63. https://doi.org/10.7326/ACPJC-2018-168-12-063.
Kim, Y., Kim, Y.S., Kim, H.Y., Noh, M.Y., Kim, J.Y., Lee, Y.J., Kim, J., Park, J., Kim, S.H., 2018. Early treatment with poly (ADP-ribose) polymerase-1 inhibitor (JPI-289) reduces infarct volume and improves long-term behavior in an animal model of ischemic stroke. Mol. Neurobiol. 55 (9), 7153–7163. https://doi.org/10.1007/s12035-018-0910-6.
Kneihsl, M., Niederkorn, K., Deutschmann, H., Enzinger, C., Poltrum, B., Fischer, R., Thaler, D., Hermetter, C., Wunsch, G., Fazekas, F., Gattringer, T., 2018. Increased middle cerebral artery mean blood flow velocity index after stroke thrombectomy indicates increased risk for intracranial hemorrhage. J. Neurointerv. Surg. 10 (9), 882–887. https://doi.org/10.1136/neurintsurg-2017-013617.
Lansberg, M.G., Cereda, C.W., Mlynash, M., Mishra, N.K., Inoue, M., Kemp, S., Christensen, S., Straka, M., Zaharchuk, G., Marks, M.P., Bammer, R., Albers, G.W., 2015. Response to endovascular reperfusion is not time-dependent in patients with salvageable tissue. Neurology 85 (8), 708–714. https://doi.org/10.1212/WNL.0000000000001853.
Liang, X., Hu, Q., Li, B., McBride, D., Bian, H., Spagnoli, P., Chen, D., Tang, J., Zhang, J.H., 2014. Follistatin-like 1 attenuates apoptosis via disco-interacting protein 2 homolog A/Akt pathway after middle cerebral artery occlusion in rats. Stroke 45 (10), 3048–3054. https://doi.org/10.1161/STROKEAHA.114.006092.
Liu, S.Q., Roberts, D., Kharitonenkov, A., Zhang, B., Hanson, S.M., Li, Y.C., Zhang, L.Q., Wu, Y.H., 2013. Endocrine protection of ischemic myocardium by FGF21 from the liver and adipose tissue. Sci. Rep. 3, 2767. https://doi.org/10.1038/srep02767.
Lopez-Morales, M.A., Castello-Ruiz, M., Burguete, M.C., Jover-Mengual, T., Aliena-Valero, A., Centeno, J.M., Alborch, E., Salom, J.B., Torregrosa, G., Miranda, F.J., 2018. Molecular mechanisms underlying the neuroprotective role of atrial natriuretic peptide in experimental acute ischemic stroke. Mol. Cell. Endocrinol. 472, 1–9. https://doi.org/10.1016/j.mce.2018.05.014.
Luo, Y., Ye, S., Chen, X., Gong, F., Lu, W., Li, X., 2017. Rush to the fire: FGF21 extinguishes metabolic stress, metaflammation and tissue damage. Cytokine Growth Factor Rev. 38, 59–65. https://doi.org/10.1016/j.cytogfr.2017.08.001.
Mao, Y., Huang, Y., Zhang, L., Nan, G., 2017. Spontaneous recanalization of atherosclerotic middle cerebral artery occlusion: case report. Medicine (Baltimore) 96 (27), e7372. https://doi.org/10.1097/MD.0000000000007372.
McBride, D.W., Zhang, J.H., 2017. Precision stroke animal models: the permanent MCAO model should be the primary model, not transient MCAO. Transl. Stroke Res. https://doi.org/10.1007/s12975-017-0554-2.
McBride, D.W., Tang, J., Zhang, J.H., 2016. Development of an infarct volume algorithm to correct for brain swelling after ischemic stroke in rats. Acta Neurochir. Suppl. 121, 103–109. https://doi.org/10.1007/978-3-319-18497-5_18.
McBride, D.W., Wu, G., Nowrangi, D., Flores, J.J., Hui, L., Krafft, P.R., Zhang, J.H., 2018. Delayed recanalization promotes functional recovery in rats following permanent middle cerebral artery occlusion. Transl. Stroke Res. 9 (2), 185–198. https://doi.org/10.1007/s12975-018-0610-6.
Navarro-Oviedo, M., Roncal, C., Salicio, A., Belzunce, M., Rabal, O., Toledo, E., Zandio, B., Rodriguez, J.A., Paramo, J.A., Munoz, R., Orbe, J., 2018. MMP10 promotes efficient thrombolysis after ischemic stroke in mice with induced diabetes. Transl. Stroke Res. https://doi.org/10.1007/s12975-018-0652-9.
Nogueira, R.G., Jadhav, A.P., Haussen, D.C., Bonafe, A., Budzik, R.F., Bhuva, P., Yavagal, D.R., Ribo, M., Cognard, C., Hanel, R.A., Sila, C.A., Hassan, A.E., Millan, M., Levy, E.I., Mitchell, P., Chen, M., English, J.D., Shah, Q.A., Silver, F.L., Pereira, V.M., Mehta, B.P., Baxter, B.W., Abraham, M.G., Cardona, P., Veznedaroglu, E., Hellinger, F.R., Feng, L., Kirmani, J.F., Lopes, D.K., Jankowitz, B.T., Frankel, M.R., Costalat, V., Vora, N.A., Yoo, A.J., Malik, A.M., Furlan, A.J., Rubiera, M., Aghaebrahim, A., Olivot, J.M., Tekle, W.G., Shields, R., Graves, T., Lewis, R.J., Smith, W.S., Liebeskind, D.S., Saver, J.L., Jovin, T.G., 2018. Thrombectomy 6 to 24 hours after stroke with a mismatch between deficit and infarct. N. Engl. J. Med. 378 (1), 11–21. https://doi.org/10.1056/NEJMoa1706442.
Otero-Ortega, L., Laso-Garcia, F., Gomez-de, F.M., Fuentes, B., Diekhorst, L., Diez-Tejedor, E., Gutierrez-Fernandez, M., 2018. Role of exosomes as a treatment and potential biomarker for stroke. Transl. Stroke Res. https://doi.org/10.1007/s12975-018-0654-7.
Pang, J., Peng, J., Matei, N., Yang, P., Kuai, L., Wu, Y., Chen, L., Vitek, M.P., Li, F., Sun, X., Zhang, J.H., Jiang, Y., 2018. Apolipoprotein e exerts a whole-brain protective property by promoting m1? Microglia quiescence after experimental subarachnoid hemorrhage in mice. Transl. Stroke Res. 9 (6), 654–668. https://doi.org/10.1007/s12975-018-0665-4.
Pena, I.D., Borlongan, C., Shen, G., Davis, W., 2017. Strategies to extend thrombolytic time window for ischemic stroke treatment: an unmet clinical need. J. Stroke 19 (1), 50–60. https://doi.org/10.5853/jos.2016.01515.
Pu, H., Jiang, X., Hu, X., Xia, J., Hong, D., Zhang, W., Gao, Y., Chen, J., Shi, Y., 2016. Delayed docosahexaenoic acid treatment combined with dietary supplementation of omega-3 fatty acids promotes long-term neurovascular restoration after ischemic stroke. Transl. Stroke Res. 7 (6), 521–534. https://doi.org/10.1007/s12975-016-0498-y.
Rai, A.T., 2015. Red pill, blue pill: reflections on the emerging large vessel stroke 'market'. J. Neurointerv. Surg. 7 (9), 623–625. https://doi.org/10.1136/neurintsurg-2015-011971.
Reis, C., Akyol, O., Ho, W.M., Araujo, C., Huang, L., Applegate, R.I., Zhang, J.H., 2017. Phase i and phase II therapies for acute ischemic stroke: an update on currently studied drugs in clinical research. Biomed. Res. Int. 2017, 4863079. https://doi.org/10.1155/2017/4863079.
Rha, J.H., Saver, J.L., 2007. The impact of recanalization on ischemic stroke outcome: a meta-analysis. Stroke 38 (3), 967–973. https://doi.org/10.1161/01.STR.0000258112.14918.24.
Salminen, A., Kaarniranta, K., Kauppinen, A., 2017a. Regulation of longevity by FGF21: interaction between energy metabolism and stress responses. Ageing Res. Rev. 37, 79–93. https://doi.org/10.1016/j.arr.2017.05.004.
Salminen, A., Kaarniranta, K., Kauppinen, A., 2017b. Integrated stress response stimulates FGF21 expression: systemic enhancer of longevity. Cell. Signal. 40, 10–21. https://doi.org/10.1016/j.cellsig.2017.08.009.
Sa-Nguanmoo, P., Tanajak, P., Kerdphoo, S., Satjaritanun, P., Wang, X., Liang, G., Li, X., Jiang, C., Pratchayasakul, W., Chattipakorn, N., Chattipakorn, S.C., 2016. FGF21 improves cognition by restored synaptic plasticity, dendritic spine density, brain mitochondrial function and cell apoptosis in obese-insulin resistant male rats. Horm. Behav. 85, 86–95. https://doi.org/10.1016/j.yhbeh.2016.08.006.
Savitz, S.I., Baron, J.C., Yenari, M.A., Sanossian, N., Fisher, M., 2017. Reconsidering neuroprotection in the reperfusion era. Stroke 48 (12), 3413–3419. https://doi.org/10.1161/STROKEAHA.117.017283.
Staiger, H., Keuper, M., Berti, L., Hrabe, D.A.M., Haring, H.U., 2017. Fibroblast growth factor 21-metabolic role in mice and men. Endocr. Rev. 38 (5), 468–488. https://doi.org/10.1210/er.2017-00016.
Sun, M., Izumi, H., Shinoda, Y., Fukunaga, K., 2018. Neuroprotective effects of protein tyrosine phosphatase 1B inhibitor on cerebral ischemia/reperfusion in mice. Brain Res. 1694, 1–12. https://doi.org/10.1016/j.brainres.2018.04.029.
Wang, Z., Leng, Y., Wang, J., Liao, H.M., Bergman, J., Leeds, P., Kozikowski, A., Chuang, D.M., 2016. Tubastatin a, an HDAC6 inhibitor, alleviates stroke-induced brain infarction and functional deficits: potential roles of alpha-tubulin acetylation and FGF-21 up-regulation. Sci. Rep. 6, 19626. https://doi.org/10.1038/srep19626.
Wang, S., Wang, Y., Zhang, Z., Liu, Q., Gu, J., 2017. Cardioprotective effects of fibroblast growth factor 21 against doxorubicin-induced toxicity via the SIRT1/LKB1/AMPK pathway. Cell Death Dis. 8 (8), e3018. https://doi.org/10.1038/cddis.2017.410.
Wang, J., Xing, H., Wan, L., Jiang, X., Wang, C., Wu, Y., 2018. Treatment targets for M2 microglia polarization in ischemic stroke. Biomed. Pharmacother. 105, 518–525. https://doi.org/10.1016/j.biopha.2018.05.143.
Wu, G., McBride, D.W., Zhang, J.H., 2018. Axl activation attenuates neuroinflammation by inhibiting the TLR/TRAF/NF-kappaB pathway after MCAO in rats. Neurobiol. Dis. 110, 59–67. https://doi.org/10.1016/j.nbd.2017.11.009.
Xie, Z., Huang, L., Enkhjargal, B., Reis, C., Wan, W., Tang, J., Cheng, Y., Zhang, J.H., 2017. Intranasal administration of recombinant Netrin-1 attenuates neuronal apoptosis by activating DCC/APPL-1/AKT signaling pathway after subarachnoid hemorrhage in rats. Neuropharmacology 119, 123–133. https://doi.org/10.1016/j.neuropharm.2017.03.025.
Xu, N., Zhang, Y., Doycheva, D.M., Ding, Y., Zhang, Y., Tang, J., Guo, H., Zhang, J.H., 2018. Adiponectin attenuates neuronal apoptosis induced by hypoxia-ischemia via the activation of AdipoR1/APPL1/LKB1/AMPK pathway in neonatal rats. Neuropharmacology 133, 415–428. https://doi.org/10.1016/j.neuropharm.2018.02.024.
Yaghi, S., Eisenberger, A., Willey, J.Z., 2014. Symptomatic intracerebral hemorrhage in acute ischemic stroke after thrombolysis with intravenous recombinant tissue plasminogen activator: a review of natural history and treatment. JAMA Neurol. 71 (9),

1181–1185. https://doi.org/10.1001/jamaneurol.2014.1210.
Ye, D., Li, H., Wang, Y., Jia, W., Zhou, J., Fan, J., Man, K., Lo, C., Wong, C., Wang, Y., Lam, K.S., Xu, A., 2016. Circulating fibroblast growth factor 21 is a sensitive biomarker for severe ischemia/reperfusion injury in patients with liver transplantation. Sci. Rep. 6, 19776. https://doi.org/10.1038/srep19776.
Yu, J., Li, X., Matei, N., McBride, D., Tang, J., Yan, M., Zhang, J.H., 2018. Ezetimibe, a NPC1L1 inhibitor, attenuates neuronal apoptosis through AMPK dependent autophagy activation after MCAO in rats. Exp. Neurol. 307, 12–23. https://doi.org/10.1016/j.expneurol.2018.05.022.
Zanette, E.M., Roberti, C., Mancini, G., Pozzilli, C., Bragoni, M., Toni, D., 1995. Spontaneous middle cerebral artery reperfusion in ischemic stroke. A follow-up study with transcranial Doppler. Stroke 26 (3), 430–433.